Journal of Quantitative Spectroscopy & Radiative Transfer 113 (2012) 2066–2071

Contents lists available at SciVerse ScienceDirect

Journal of Quantitative Spectroscopy & Radiative Transfer

journal homepage: www.elsevier.com/locate/jqsrt

Optical–optical double resonance circular polarization spectroscopy: Measurement of the disorientation cross section in $6p^2P_{1/2}$ Cs atoms

S.B. Bayram [a,*], D.S. Fisher [a], O. Popov [a], Z. Sağlam [b]

[a] Department of Physics, Miami University, Oxford, OH 45056, USA
[b] Department of Physics, Faculty of Science, Aksaray University, Aksaray, Turkey

ARTICLE INFO

Article history:
Received 10 September 2011
Received in revised form
14 June 2012
Accepted 19 June 2012
Available online 27 June 2012

Keywords:
Spectroscopy
Atom–atom collisions
Disorientation
Inelastic collisions
Cross section
Radiative transfer

ABSTRACT

We have measured the cross section for the disorientation of excited $6p^2P_{1/2}$ ^{133}Cs atoms by collisions with ground state Ar atoms by optical–optical double resonance circular polarization spectroscopy. Circular polarization spectra were measured for the $6s^2S_{1/2} \rightarrow 6p^2P_{1/2} \rightarrow 10s^2S_{1/2}$ transition. Orientation was optically induced in the $^2P_{1/2}$ state by circularly polarized light. A polarization degree was measured when two pulsed lasers were circularly polarized with the same helicities and opposite helicities, respectively. The intensity of the cascade fluorescence signal, monitored from the $9p^2P_{1/2} \rightarrow 6s^2S_{1/2}$ transition at 361.73 nm, was analyzed in the presence of Ar pressures ranging from 7 mbar to 133 mbar. This is a direct measure of the importance of the orientation to inelastic process in alkali rare-gas collisions. A disorientation cross section value of 9.25 (1.4) Å^2 was extracted from the measurements. Our result is in good agreement with the theoretical and experimental predictions within the error limits.

1. Introduction

Investigation of atomic collisions with neutral atoms, molecules, and ions is a key to understand energy and energy transfer processes, and depolarization due to collisional disorientation of electronic moments [1–3]. Disorientation and associated disorientation cross sections offer valuable information to understand the anisotropic interaction between atoms in collision [4–8]. In particular, dynamical information about the state multipoles, a description of the intermediate levels of the collision complex, anisotropic molecular potentials, energy and charge transfer processes, can all be deduced from investigation of collisional studies [9–11,2]. Experimental investigations of disorientation cross section in the $6p^2P_{1/2}$ state cesium atoms, up to now, were carried out using incoherent light sources as optical excitation [12,13]. Gallagher [14] studied collisional depolarization in the cesium resonance states using the Hanle-effect at zero field while Bulos and Happer [15], using the same technique, incorporated the effect of nuclear spin on the Hanle-effect signal. Guiry and Krause [16], using a Zeeman-scanning technique at high magnetic field, showed discrepancy between the Hanle-effect and their Zeeman-scanning results. The depolarization cross sections measured by Refs. [14,16] differ by a factor of 10, and Refs. [15,16] differ by a factor of 2. This work is motivated by the insufficient data available to compare with the Zeeman-scanning and Hanle-effect techniques. Thus, we have experimentally studied the orientation-dependent collisional cross section of the Cs $6p^2P_{1/2}$ atoms based on optical–optical double-resonance circular polarization spectroscopy using a pump–probe laser technique.

In this paper, a circular polarization degree was measured at Ar gas pressures ranging from 7 mbar to 133 mbar. The measured circular polarization degree is strongly dependent on orientation since only the $J = \frac{1}{2}$ state can be purely oriented. The disorientation cross section is extracted from the circular polarization measurements. Our measurements differ from the Hanle-effect and Zeeman-scanning

* Corresponding author.
E-mail address: bayramsb@muohio.edu (S.B. Bayram).

0022-4073/$ - see front matter © 2012 Elsevier Ltd. All rights reserved.
http://dx.doi.org/10.1016/j.jqsrt.2012.06.017

techniques and are sensitive to the relative polarization directions of the pump and probe pulsed lasers.

In the following sections, we provide a basic description of the excited state multipoles and the polarization as a function of orientation induced in the excited state, and our experimental apparatus and techniques. In Section 4, we present the results and rate equation analysis of how to derive disorientation cross section from the measurements.

2. Excited state multipoles and circular polarization

The excitation of an ensemble of atoms is done through the $6s^2S_{1/2} \rightarrow 6p^2P_{1/2} \rightarrow 10s^2S_{1/2}$ transition. The excited $^2P_{1/2}$ state can be purely oriented by optically pumping with circularly polarized light and can be characterized by describing the distribution of atoms over the Zeeman sublevels.

2.1. Excited state multipoles in the $J=\frac{1}{2}$ level

We consider an ensemble of atoms that is initially in a ground state, and then is excited to a state with $J=\frac{1}{2}$ using circularly polarized light. Assuming a quantization axis (z-axis) defined by the propagation direction of the circularly polarized light, the transition between ground and excited magnetic sublevels occurs with $\Delta m=+1$ or $\Delta m=-1$ depending on the helicity of the circularly polarized light, positive or negative, respectively. Then, a population imbalance in the $\pm m$ sublevels can be created by an absorption of circularly polarized light under the selection rule $\Delta m=\pm 1$. The $^2P_{1/2}$ state can be characterized by describing the distribution of atoms over the Zeeman sublevels. To describe the anisotropic angular momentum distribution in the excited state by means of absorption or emission of polarized light a spherical tensor formalism has been developed [17,18]. From the spherical tensor formalism, atomic polarization has been expressed in terms of the irreducible tensor components of the density matrix elements [19,20]. Although there are four tensor components $(2J+1)^2$, symmetry relations can be used to reduce the number of nonzero components. Since our system is cylindrically symmetric about the quantization axis, only zeroth-components of the multipoles survive. There is one axially symmetric multipole with the highest rank up to $k=2J=1$ in the excited $J=\frac{1}{2}$ state, which can be specified by the zeroth-components of monopole moment of rank $k=0$ (*population*), and dipole moment of rank $k=1$ (*orientation*). Thus, the ensemble of $J=\frac{1}{2}$ atoms can be characterized in terms of population and orientation over the Zeeman sublevels. It is important to note that spontaneous emission can generate coherences but these coherences are averaged out over the ensemble of atoms, and thus coherences are not generated among the Zeeman sublevels. Thus, coherences need not be considered for any theoretical and experimental argument described in this work.

The orientation can be defined in terms of the angular momentum quantum numbers [19,20] as

$$\langle O_o \rangle = \frac{\langle J_z \rangle}{\sqrt{J(J+1)}} = \sum_m |\sigma(m)|^2 \frac{m}{\sqrt{J(J+1)}} \tag{1}$$

where J is the total angular momentum of the excited state and $\sigma(m)$ is a Clebsch–Gordan coefficient. The spatial distribution of angular momenta in the $^2P_{1/2}$ state can be purely oriented by circularly polarized light. Thus, using Eq. (1), orientation can be calculated as $1/\sqrt{3}$ for the $J=\frac{1}{2}$ state. The intensity of the fluorescence radiation can be written in terms of orientation [20] as,

$$I(\phi,\theta,\chi) = \frac{I_0}{3}\left\{1-\frac{3}{2}h^{(1)}(JJ') \times \langle O_o \rangle \cos\theta \sin 2\beta\right\} \tag{2}$$

where (ϕ,θ,χ) are Euler angles relating the collision frame to the detector frame, I_o is the total intensity, $\beta=\pm\pi/4$ for circularly polarized light, and $h^{(1)}(JJ')$ is a function that depends only on the angular momentum of the excited $6p^2P_{1/2}$ state and the final $10s^2S_{1/2}$ state. Thus, for the $6s^2S_{1/2} \rightarrow 6p^2P_{1/2} \rightarrow 10s^2S_{1/2}$ transition, $h^{(1)}(JJ')$ has a value of $2/\sqrt{3}$ [20]. Since our system has cylindrical symmetry the azimuthal angle ϕ is irrelevant and θ is the angle between the quantization axis and the propagation direction of the second laser. Thus, $\cos\theta=1$. In our experiment, the helicity of laser 1 was kept positive while the helicity of laser 2, responsible for the $6p^2P_{1/2} \rightarrow 10s^2S_{1/2}$ transition, was alternately changed from positive to negative with respect to the helicity of laser 1. Thus, a general definition for the circular polarization can be written as

$$P_c = \frac{I(\beta=\pi/4)-I(\beta=-\pi/4)}{I(\beta=\pi/4)+I(\beta=-\pi/4)} \tag{3}$$

Substituting Eq. (2) into Eq. (3), one can express the circular polarization in terms of orientation $\langle O_o \rangle$ as

$$P_c = \sqrt{3}\langle O_o \rangle \tag{4}$$

One can calculate the circular polarization degree for the $6s^2S_{1/2} \rightarrow 6p^2P_{1/2} \rightarrow 10s^2S_{1/2}$ transition as $P_c=1$ (100%) in the absence of depolarization effects by substituting Eq. (1) into Eq. (4). Also, orientation in terms of measured P_c can be defined by inverting Eq. (4) as

$$\langle O_o \rangle = \frac{P_c}{\sqrt{3}} \tag{5}$$

It is important to note that the orientation is expected to be altered by the hyperfine interaction which in return decreases the polarization degree. The consideration of the amount of hyperfine reduction will be discussed in a later section of the paper.

3. Experimental technique

A schematic overview of the experimental apparatus is shown in Fig. 1. A pulsed neodymium-doped yttrium aluminum garnet (Nd:YAG) laser, operating at 532 nm with an average power of 1 W and a pulse repetition rate of 20 Hz, is used to pump two home-built tunable dye lasers and one dye laser amplifier. The pulse width was measured to be approximately 6.5 ns using a 0.2-ns rise-time ultrafast photodetector. Dye laser oscillators are constructed using a grazing incidence type in a Littman–Metcalf cavity design. Dye laser 1 uses a dye circulating system to maintain the power at 0.03 mW and excites the $6p^2P_{1/2}$ state at 894.35 nm. Dye laser 2 uses a single stage

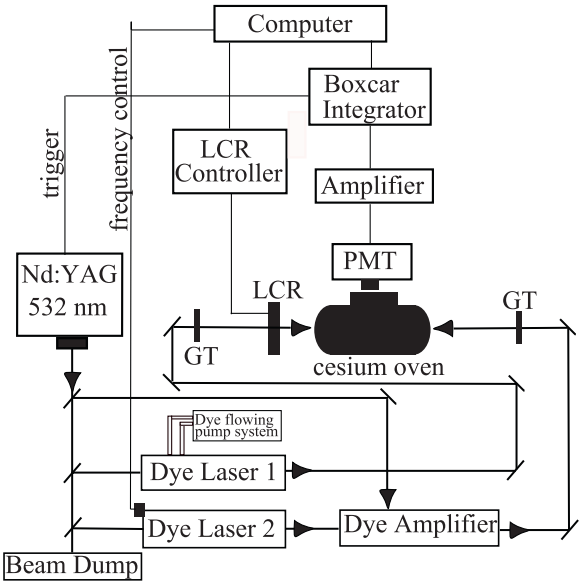

Fig. 1. A schematic diagram of the experimental apparatus. GT, Glan–Thompson prism polarizer; LCR, liquid-crystal variable retarder; PMT, photo-multiplier tube.

dye laser amplification system which increases the output power of the dye by about a factor of 5 and so generates an average power of 0.2 mW. Dye laser 2 excites the final $10s^2S_{1/2}$ state at 583.88 nm.

Both lasers are strongly linearly polarized using Glan–Thompson prism polarizers with extinction ratios of better than 10^{-5}. Then, a high quality quarter-wave plate in the pump laser beam path is used to produce circular polarization with negative helicity σ^-. A temperature- and remote-controlled liquid crystal variable retarder with an extinction ratio of 10^{-3} was used in the probe beam path in order to alternately produce circular polarization with σ^- and σ^+ helicities. The oven has a sealed Pyrex cell containing Cs with background pressure of about 10^{-8} mbar. A resistively heated, nonmagnetic aluminum oven was used to heat the cell. The oven was wrapped with an aluminum oxide blanket to maintain the temperature at about 70 °C with the uncertainty under 1 °C by a temperature controller.

The intensity of the cascade fluorescence from the $9p^2P_{1/2}$ state to the ground $6s^2S_{1/2}$ state was recorded at 361.73 nm by using a UV sensitive photomultiplier tube (PMT), which uses a combination of interference and color glass filters in order to eliminate background due to scattered and atomic resonance fluorescence. A partial energy level diagram of the excitation scheme is illustrated in Fig. 2. The signals were detected when the helicities of the lasers are the same ($\sigma^-\sigma^-$) and opposite ($\sigma^-\sigma^+$) to each other. The output of the PMT signal was amplified using a two stage amplifier and processed in a boxcar integrator/averager with a 166-ns gate-width, opened after a 1 ns delay following the laser pulses, operating in a 100-sampling mode, where the average single-shot level within the detection gate is digitized. Our typical signal size is about 10^3 photons for each laser pulse. The digitized signals ere stored on a computer using a LabVIEW program while

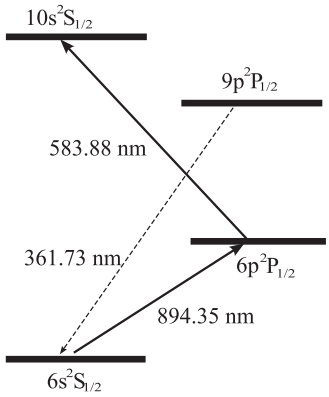

Fig. 2. Some of the important transitions for the double resonance and their corresponding wavelengths are shown in solid line, the cascade fluorescence channel observed in the experiment is shown in dotted line.

monitoring the signal within the gate-width in real time using a 500 MHz, 2 GSa/s digital oscilloscope. In the experiment, disorientation induced by atomic collisions between the $6p^2P_{1/2}$ Cs atoms and ground state Ar atoms at pressures ranging from 7 mbar to 133 mbar was measured by optical–optical double-resonance circular polarization spectroscopy. Then, a disorientation cross section was extracted from the measurement.

4. Results and discussion

The possible systematic effects that tend to reduce the measured circular polarization degree are radiation trapping, nonlinear processes due to higher laser power, and unobserved hyperfine structure in the excited state of Cs. Thus, we have measured the lifetime of the excited state and found that the radiation trapping at the experimental cell temperature (70 °C) has a negligible effect on the excited state. For ^{133}Cs atoms with nuclear spin $I=7/2$, the nuclear spin couples with the electronic angular momentum, $J=\frac{1}{2}$ in this case, and initiates precession between I and J about a new total angular momentum F. This precession perturbs and depolarizes the excited state by a factor of $g^{(1)}$, the so-called hyperfine depolarization coefficient [21,22]. However, if the temporal overlap time of the pulses can be made much less than the smallest hyperfine precession time, one can possibly freeze out the electronic orientation in the excited state. That is, the atoms are promoted to the final state by the two-step excitation before the hyperfine precessional motion in the intermediate state can take place. Thus, for atoms with nonzero nuclear spin, it is important to know the pulse width and the temporal overlap time of the pulses in order to determine the temporal resolution. The measurement of the exact time delay between the dye laser pulses, measured with two photodiodes triggered by the YAG laser, gives the overlap time. We have also confirmed this measurement with direct beam path measurements. The temporal overlap time of the dye lasers is measured to be 2.53 ns which is bigger than the inverse of the highest hyperfine frequency component in the excited state (0.86 ns). In this case, electronic orientation is expected to

be perturbed by the hyperfine interaction which in return decreases the circular polarization degree. The $g^{(1)}$ coefficient for ^{133}Cs $6p^2P_{1/2}$ state is given in [23] as 0.344. Thus, Eq. (4) can be re-written as $P_c=\sqrt{3}\langle O_o\rangle g^{(1)}$. In this case, we expect the circular polarization to be $P_c=-0.34$ (-34%).

We have also considered systematic effects due to magnetic fields. Some of the important magnetic fields may be the Earth's magnetic field and magnetic field produced by current carrying the power cables around the experimental apparatus. The precession frequency due to Earth magnetic field in the $6p^2P_{1/2}$ state is 0.496 MHz and the frequency due to the overlap time of the pulsed lasers is about 395.2 MHz. Thus, the phase change between them is as small as 7.88×10^{-3} rad. We have also estimated the maximum precession frequency for the possible systematic effects due to magnetic fields created by other sources such as power cables and heating elements and found this frequency to be about 0.2 MHz. The highest hyperfine precession frequency in the $6p^2P_{1/2}$ state is 1.167 GHz. Comparing the total background frequency with the highest hyperfine precession frequency, systematic effects are negligible and have no effect on the polarization measurements.

We have also checked for the existence of external perturbations such as the influence of laser power and temperature dependence on the measured polarization degree. Measurements for the $6s^2S_{1/2}\rightarrow 6p^2P_{1/2}\rightarrow 10s^2S_{1/2}$ transition confirm that systematic effects do not alter the orientation produced in the $6p^2P_{1/2}$ state. We measured the circular polarization degree as $P_c=-32\pm3\%$ with a cesium cell containing no buffer gas. We summarized in Table 1 calculated and measured values of orientation in the $6p^2P_{1/2}$ and circular polarization degree. Our results show good agreement with the theoretical calculations.

4.1. Rate equation analysis to extract collisional cross section

Optical pumping to the $m=-\frac{1}{2}$ Zeeman sublevel of the $6p^2P_{1/2}$ state can be achieved by a circularly polarized laser according to the selection rule $\Delta m=-1$. The population in the $6p^2P_{1/2}$ Zeeman sublevels is collisionally modified in collisions with ground state argon atoms. Collisional mixing among the $m=\pm\frac{1}{2}$ sublevels reduces the amount of orientation produced in the excited state. The population ($N_J, J=\pm\frac{1}{2}$) variations among the Zeeman sublevels can be conveniently expressed by a theoretical model using the rate equations analysis [24,19] as

$$\dot{N}_{1/2}=-(\gamma+\Gamma_1)N_{1/2}+\Gamma_2N_{-1/2} \tag{6}$$

$$\dot{N}_{-1/2}=-(\gamma+\Gamma_2)N_{-1/2}+\Gamma_1N_{1/2}+\Gamma_p \tag{7}$$

Table 1
Calculated and measured values of orientation in the $^2P_{1/2}$ state and circular polarization degree for the $6s^2S_{1/2}\rightarrow 6p^2P_{1/2}\rightarrow 10s^2S_{1/2}$ transition.

$\langle O_o\rangle_{\text{cal.}}$	$\langle O_o\rangle_{\text{meas.}}$	$(P_c)_{\text{cal.}}$	$(P_c)_{\text{meas.}}$
-0.57	$-0.54(5)$	-34%	$-32\pm3\%$

where Γ_p is the pump pulse rate and γ is the radiative decay rate. The net rate of change of the total density N and orientation $\langle O_o\rangle$ in the excited state can be defined as

$$\dot{N}(t)=-\gamma N+\Gamma_p \tag{8}$$

and

$$\langle\dot{O}_o\rangle=-\gamma_o\langle O_o\rangle-\Gamma_p/\sqrt{3} \tag{9}$$

where $\gamma_o=\gamma+2\Gamma_1$ is the orientation decay rate. Here, $\Gamma_o=2\ \Gamma_1$ is responsible for the collisional mixing and contains information about the gas-kinetic cross section. The principle of detailed balance allows one to write $\Gamma_1=\Gamma_2$. The time-dependent solutions of the total population and orientation can be derived as

$$N(t)=\frac{\Gamma_p}{\gamma}(1-e^{-\gamma t}) \tag{10}$$

and

$$\langle O_o(t)\rangle=\frac{\Gamma_p}{\sqrt{3}\gamma_o}(1-e^{-\gamma_o t}) \tag{11}$$

Note that the steady-state value of the total population density N at $t=\infty$ is Γ_p/γ. We can define population in each magnetic sublevel in terms of the total population and orientation for the $J=\frac{1}{2}$ atoms as

$$N_{1/2}(t)=\tfrac{1}{2}N(t)+\tfrac{\sqrt{3}}{2}\langle O_o(t)\rangle \tag{12}$$

$$N_{1/2}(t)=\tfrac{1}{2}N(t)-\tfrac{\sqrt{3}}{2}\langle O_o(t)\rangle \tag{13}$$

Thus, circular polarization in terms of the measured signals, integrated over the temporal overlap time of the pulses, can be written as

$$P_c=\frac{S^{\sigma^-}-S^{\sigma^+}}{S^{\sigma^-}+S^{\sigma^+}}=\frac{\int_0^T N_{-1/2}(t)-\int_0^T N_{1/2}(t)}{\int_0^T N_{-1/2}(t)+\int_0^T N_{1/2}(t)} \tag{14}$$

where S^{σ^-} and S^{σ^+} refer to the signals when the helicities of the lasers are $\sigma_1^-\sigma_2^-$ and $\sigma_1^-\sigma_2^+$, respectively. In this expression, labels 1 and 2 refer to laser 1 and laser 2. Eq. (14) allows one to express the circular polarization with the presence of hyperfine depolarization coefficient $g^{(1)}$, multiplied by the orientation, in terms of disorientation cross section and argon gas pressure as

$$P_c=\frac{\gamma}{\gamma_o}\frac{T+\dfrac{1}{\gamma_o}(e^{-\gamma_o T}-1)}{T+\dfrac{1}{\gamma}(e^{-\gamma T}-1)}g^{(1)} \tag{15}$$

The disorientation cross section can be defined using gas-kinetic cross section relations as

$$\Gamma_o=\rho_{\text{Ar}}\sigma_o\overline{v}_{\text{CsAr}} \tag{16}$$

where ρ_{Ar} is the ratio of the argon gas pressure to the thermal energy constant kT, and σ_o is the disorientation cross section. In Eq. (16), we denoted $\langle v\rangle$ as $\overline{v}_{\text{Cs-Ar}}$ which is the average velocity of the colliding cesium and argon atoms over the Maxwell–Boltzmann distribution of relative velocities at the operating cell temperature. Eq. (15) provides connection between the experimentally measured circular polarization degree P_c in relation to the argon gas pressure and the disorientation cross section. Fig. 3 shows

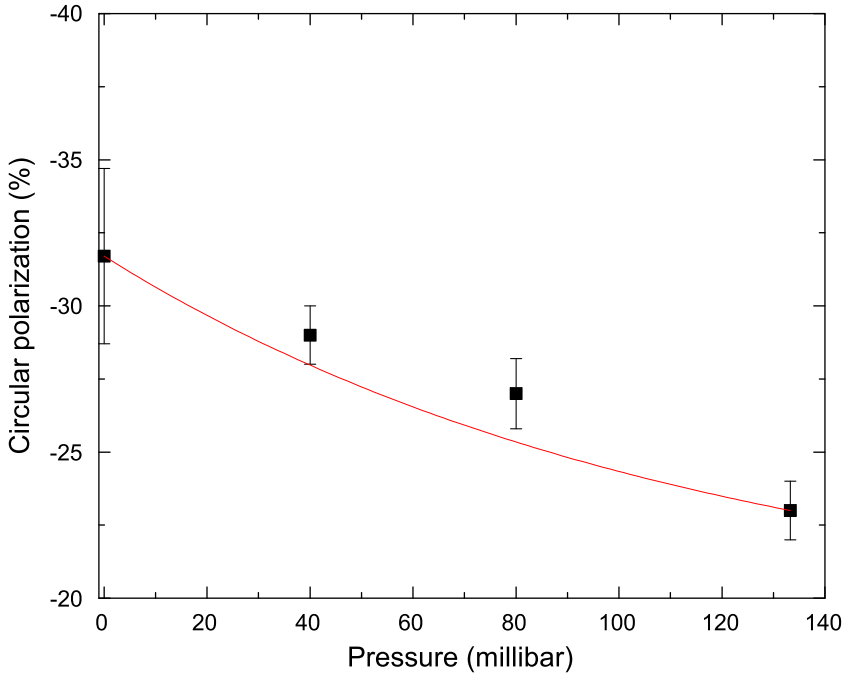

Fig. 3. Nonlinear least square fit of the circular polarization degree as a function of Ar gas pressure for the two-step double-resonance $6s^2S_{1/2} \rightarrow 6p^2P_{1/2} \rightarrow 10s^2S_{1/2}$ transition.

the circular polarization degree as a function of argon gas pressures ranging from 7 mbar to 133 mbar.

Thus, the disorientation cross section value, extracted from the nonlinear-least square fit of the experimental results, is in excellent agreement with the theoretical [26] and experimental [16] values. These are summarized in Table 2. For the rate equation analysis of the $6p^2P_{1/2}$ state population, the laser pulse temporal profile was modeled as rectangular pulses. Other pulse shapes may be used and lead to negligibly different polarization results [9,25,10].

First, we now discuss the various results shown in Table 2. Hanle-effect linewidths studied by [14] were altered by the nuclear spin effect which was not taken into consideration when reporting the collisional cross section. This omission led to a considerable underestimate of the disorientation cross section value. Bulos and Happer [15] have showed the evidence of the nuclear spin effect on pressure-broadened Hanle signal and treated their results accordingly. A disorientation cross section was determined by [16] using a Zeeman scanning technique and the results showed that at low magnetic field nuclear spin coupled with electronic angular momentum while at sufficiently high magnetic field ($\sim$ 10 kG) nuclear spin and angular momentum decoupled. The decoupling due to high magnetic field resulted in higher cross section value. Thus, depolarization cross section measurement done by [16] is larger by a factor of 10 than depolarization cross section value reported by [14]. Also, the cross section value reported by [16] is higher than the same value reported by [15]. Although there is a possibility of collisional mixing of the $^2P_{1/2}$ and $^2P_{3/2}$ states in a high magnetic field, the influence of the mixing on the polarization measurement reported by [16] was negligible. It has been pointed out that the disorientation cross section may exhibit variations of up to 50%, depending on the model chosen to represent the collisional mixing process [12]. The experimental cross sections reported by [16] and this work are in good agreement with the theoretical cross section, calculated by [26] without assuming the presence of a high magnetic field.

Table 2
Disorientation cross section σ_1 due to inelastic collisions between $6p^2P_{1/2}$ Cs and ground state Ar atoms are listed. TPS: Two-step polarization spectroscopy using Nd:YAG pulsed laser, ZeS: Zeeman scanning technique at high magnetic field, HaE: Hanle Effect at zero magnetic field.

$\sigma_1(\text{Å}^2)$	Method	Reference
9.25(1.4)	TPS	This work
10.7(0.6)	ZeS	[16]
9.3	Theory	[26]
1.7	HaE	[14]
5.0(1.0)	HaE	[15]

5. Conclusions

We present in this paper results of measurements of the collisional cross section in $6p^2P_{1/2}$ cesium atoms using a pump–probe, optical–optical double resonance circular polarization spectroscopy technique. We measured the orientation-dependent polarization as a function of Ar gas pressure ranging from 7 mbar to 133 mbar. The circular polarization of the $6s^2S_{1/2} \rightarrow 6p^2P_{1/2} \rightarrow 10s^2S_{1/2}$ transition is found to be independent of the laser power, temperature, and variation in the intensity of the fluorescence signal. Depolarization for the ^{133}Cs $6p^2P_{1/2}$ atoms in collision with ground state Ar atoms is evident on the orientation-dependent circular

polarization data. From the measurements, a disorientation cross section value of 9.25(1.4) $Å^2$ is obtained. Our result is in good agreement with the theory [26] and with Ref. [16] within the error limits.

Acknowledgments

The financial support of the Research Corporation under the Grant number CC7133 and Miami University, College of the Arts and Sciences are acknowledged.

References

[1] Baylis WE. Collisional depolarization in the excited state. In: Hanle W, Kleinpoppen H, editors. Progress in atomic spectroscopy part B. New York: Plenum; 1979. p. 1227–97.
[2] Zhao LB, Watanabe A, Stancil PC, Kimura M. Ab initio investigation of electron capture by Cl^{7+} ions from H. Phys Rev A 2007;76: 022701–1-022701-8.
[3] Andersen N, Bartschat K. Polarization, alignment, and orientation in atomic collisions. New York: Springer-Verlag; 2001.
[4] Kaupp H, Didra H-P, Kramer C, Baumann MC. Collisional depolarization of excited $^{114}Cd5s5p\,^3P_1$ atoms by collisions with molecular gases. Z Phys D 1993;27:307–12.
[5] Costen ML, McKendrick KG. Orientation and alignment moments in two-color polarization spectroscopy. J Chem Phys 2005;122: 164309–20.
[6] Costen ML, Crichton HJ, McKendrick KG. Measurement of orientation and alignment moment relaxation by polarization spectroscopy: theory and experiment. J Chem Phys 2004;120:7910–26.
[7] Bayram SB, Kin S, Welsh MJ, Hinkle JD. Collisional depolarization of Zeeman coherences in the $^{133}Cs6p^2P_{3/2}$ level: double-resonance two-photon polarization spectroscopy. Phys Rev A 2006;73: 042713–1-042713-6.
[8] Bayram SB, Koirala P. Polarization spectroscopy to determine alignment depolarization of the $^{133}Cs6p^2P_{3/2}$ atoms using a pump–probe laser technique. Opt Commun 2009;282:1567–73.
[9] Cook L, Olsgaard D, Havey M, Sieradzan A. Collisional modification of the atomic-Na $3s^2S_{1/2}-5s^2S_{1/2}$ two-color two-photon polarization spectrum. Phys Rev A 1993;47:340–5.
[10] Lasell R, Bayram SB, Havey MD, Kupriyanov DV, Subbotin SV. Polarization-dependent Mg $(3p^1P_1-5s^1S_0,4d^1D_2)$-rare-gas-atom excited-state optical collisions: experiment and theory. Phys Rev A 1997;56:2095–108.
[11] Wong TH, Kleiber PD. Evolution of the electronic orbital alignment in metal-atom-rare-gas fractional collisions. Phys Rev A 1998;57: 2227–30.
[12] Guiry J, Krause L. Depolarization of $6^2P_{3/2}$ cesium atoms, induced in collisions with noble gases. Phys Rev A 1976;14:2034–42.
[13] Fricke J, Haas J, Lüscher E. Cross sections for excited-state mixing in cesium-noble-gas collisions from D_2 optical pumping. Phys Rev 1967;163:45–53.
[14] Gallagher A. Collisional depolarization of the Rb 5p and Cs 6p doublets. Phys Rev 1967;157:68–72.
[15] Bulos BR, Happer W. Nuclear-spin inertia and pressure broadening of $^2P_{1/2}$ Hanle-effect signals. Phys Rev A 1971;4:849–53.
[16] Guiry J, Krause L. m_j mixing in oriented $6^2P_{1/2}$ cesium atoms, induced in collisions with noble gases. Phys Rev A 1972;6:273–7.
[17] Fano U. Description of states in quantum mechanics by density matrix and operator techniques. Rev Mod Phys 1957;29:74–93.
[18] Fano U, Macek JH. Impact excitation and polarization of the emitted light. Rev Mod Phys 1973;45:553–73.
[19] Blum K. Density matrix theory and applications. New York: Plenum; 1981.
[20] Greene CH, Zare RN. Photofragment alignment and orientation. Ann Rev Phys Chem 1982;33:119–50.
[21] Zare RN. Angular momentum: understanding spatial aspects in chemistry and physics. New York: Wiley; 1988.
[22] Arimondo E, Inguscio M, Violino P. Experimental determinations of the hyperfine structure in the alkali atoms. Rev Mod Phys 1977;49:31–75.
[23] Havey MD, Vahala LL. Comment on orientation, alignment and hyperfine effects on dissociation of diatomic molecules to open shell atoms. J Chem Phys 1987;86:1648–9.
[24] Blushs K, Auzinsh M. Validity of rate equations for Zeeman coherences for analysis of nonlinear interaction of atoms with broadband laser radiation. Phys Rev A 2004;69:063806–14.
[25] Lasell R, Olsgaard DA, Bayram SB, Havey MD, Kupriyanov DV. Polarization spectra of excited-state-M g(3p)-rare-gas-atom optical collisions. Phys Rev A 1994;50:423–8.
[26] Gordeyev EP, Nikitin EE, Ovchinnikova MYa. Calculation of cross sections for the depolarization of ^2P states in alkali atoms. Can J Phys 1969;47:819–1827.